Journal of Applied Polymer Science

Synthesis and Characterization of an Associative Polymer with an Octylphenyl Polyoxyethylene Side Chain as a Potential Enhanced-Oil-Recovery Chemical

Zhongbin Ye,[1,2] Xuan Zhang,[2] Hong Chen,[1] Lijuan Han,[1,2] Chao Lv,[2] Zheng Su,[1] Jiarong Song[2]

[1]State Key Laboratory of Oil and Gas Reservoir Geology and Exploitation, Southwest Petroleum University, Chengdu 610500, People's Republic of China

[2]School of Chemistry and Chemical Engineering, Southwest Petroleum University, Chengdu 610500, People's Republic of China

Correspondence to: X. Zhang (E-mail: zx85917@hotmail.com)

A novel nonionic surfmer, AGE-TX-100, was synthesized by the epoxide ring-opening reaction of allyl glycidyl ether and polyoxyethylene (10) octylphenyl ether (TX-100). Then a novel copolymer, acrylamide (AM)/acrylic acid (AA)/AGE-TX-100, was synthesized with AM, AA, and AGE-TX-100 in aqueous solution through free-radical random polymerization. The structures of the novel surfmer and copolymer were characterized by IR and ^{1}H-NMR. The results of the salt-resistance tests and the rheological tests indicate that the copolymer had good salt tolerance, thermal stability at high temperatures, and shearing resistance under high shear rates. The environmental scanning electron micrographs showed that the copolymer could form a tighter three-dimensional network structure than partially hydrolyzed polyacrylamide (HPAM) in aqueous solution. Compared with the HPAM solution, the copolymer solution showed a good ability to emulsify organic components. © 2014 Wiley Periodicals, Inc. J. Appl. Polym. Sci. **2014**, *131*, 41024.

KEYWORDS: copolymers; functionalization of polymers; oil & gas; rheology; surfactants

Received 3 April 2014; accepted 12 May 2014

DOI: 10.1002/app.41024

INTRODUCTION

After primary and secondary recovery, only 20–50% of crude oil can be extracted from reservoirs,[1–4] and 50–80% of crude oil is still absorbed on the surface of the rocks in underground.[5–7] With the depletion of gas and crude oil reservoirs and the sharp consumption of fossil energy,[8] much attention has been paid to the investigation of new ways[9–12] to squeeze extra barrels from the remaining crude oil in these mature oil fields by various enhanced oil recovery (EOR) techniques, such as thermal recovery, gas injection, miscible flooding, microbial injection, and chemical injection.[13]

Chemical injection with polymers, such as polymer flooding,[14–16] polymer–surfactant flooding,[17,18] and alkali–polymer–surfactant flooding,[19–22] is one efficient type of EOR technology that reduces the mobility between water and crude oil, and improves oil recovery in old oil fields. In addition, in recent years, these technologies have been applied to other difficult to explore reservoirs, such as offshore oil fields, heavy oil pools, and reservoirs with higher temperatures and salinities.[23,24]

In chemical flooding systems, partially hydrolyzed polyacrylamide (HPAM) has been widely applied as a rheology control agent because, with it, one can achieve a high viscosity by increasing the molecular weight of HPAM in aqueous solution. However, the viscosity of HPAM solution can be easily and sharply reduced under the harsh conditions of high salinity, high temperature, and high shear rate.[25–29]

To solve these problems in chemical flooding systems, in recent decades, hydrophobically associating polyacrylamide (HAPAM) has been developed in oil fields. Compared with HPAM, HAPAM contains a small number of hydrophobic groups in its structure (<1%) that are distributed along the hydrophilic chains in blocks or at random in its structure.[30–33] HAPAM can form a reversible three-dimensional supermolecular network structure via the hydrophobic groups in aqueous solution and build a high viscosity. In addition, HAPAM solution can exhibit excellent shearing stability, temperature resistance, and salt tolerance because of the intermolecular association.[34–39] At present, HAPAM has been successfully applied as a mobility control agent for EOR chemicals.[40,41]

However, there exist some difficulties in the synthesis of HAPAM. One of these problems is the insolubility of hydrophobic macromonomers in water.[42] Many researchers have used micellar copolymerization techniques to solve this problem. During the synthesis process, surfactants are added as emulsifiers to the reaction solution to ensure the solubility and stability of the hydrophobic macromonomer in the micelles.[42–46] However, the

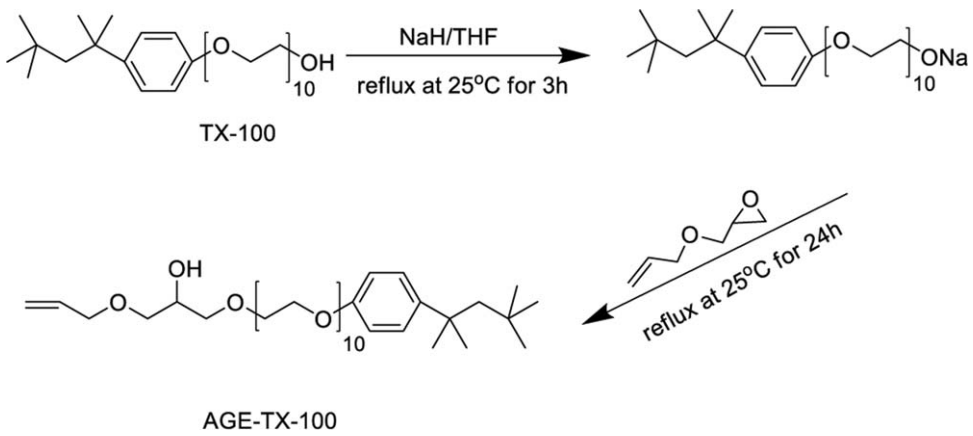

Scheme 1. Synthesis route of the surfmer AGE-TX-100.

addition of surfactants may results in some side effects,[42,47,48] such as chain transfer that leads to a low molecular weight and difficulties in the removal of the emulsifiers after the copolymerization. New ways to get past these defects are still needed.

A polymerizable surfactant, or *surfmer,* is one type of functional surfactant that not only contains a hydrophobic tail and hydrophilic head group but also has polymerizable vinyl double bonds.[49–53] These emulsifiers are widely used for preparing vesicles for functional polymer latexes, soft templates for synthesizing organized nanomaterials, biological simulation, and so on.[54–57] Because of their special amphiphilic molecular structures, polymerizable surfactants can also be used as hydrophobic monomers to synthesize HAPAM and overcome the drawbacks during the micellar copolymerization. Although there are some reports on the synthesis of HAPAM with surfmers, most of these studies are about cationic surfmers,[58–60] and the studies of HAPAM containing a nonionic surfactant structure are very scarce. In addition, polymers containing cationic structures with a high concentration that may cause a higher cost during the EOR processes may be needed, as cationic polymers can be adsorbed on the rock surface and the concentration of polymer was finally reduced; this is due to the negative charge on the rock surface.

In this study, a novel nonionic surfmer, AGE-TX-100, was synthesized by the epoxide ring-opening reaction of allyl glycidyl ether and polyoxyethylene (10) octylphenyl ether (TX-100). Then, a novel copolymer, acrylamide (AM)/acrylic acid (AA)/AGE-TX-100, was synthesized with AM, AA, and AGE-TX-100 in aqueous solution through free-radical random polymerization. The structures of the surfmer and copolymer were characterized by IR and ^{1}H-NMR. The synthesis conditions were optimized. The solution properties of the AM/AA/AGE-TX-100 copolymer were investigated; these properties included the salt resistance, thermal stability, and shearing tolerance. In addition, with the incorporation of TX-100 in the polymer chain, the emulsifying ability of the copolymer was also investigated.

EXPERIMENTAL

Materials

AM was recrystallized twice from chloroform, and AA was purified by distillation under reduced pressure. Tetrahydrofuran (THF) was dried with anhydrous sodium hydroxide (NaOH) before use. Allyl glycidyl ether, purchased from Chengdu Xiya Chemicals Co., Ltd. (China), and ammonium persulfate, TX-100, sodium chloride (NaCl), magnesium chloride hexahydrate, and calcium chloride anhydrous, obtained from Chengdu Kelong Chemicals Co., Ltd. (China), were all analytically pure and were used without further purification. The cationic surfmer hexadecyl dimethyl allyl ammonium chloride (C_{16}DMAAC) provided by Feixiang Co. were industrial pure and used without further purification. Water was filtered and deionized in an ultrapure water system.

Synthesis of Surfmer AGE-TX-100

TX-100 (31.25 g, 50 mmol) and 50 mL of dry THF were added to a 250-mL, three-necked flask, and NaH (1.44 g, 60 mmol) was then added to the flask. After the mixture was stirred for 3 h at 25°C under a nitrogen atmosphere, the solution of allyl glycidyl ether (5.71 g, 50 mmol) in 50 mL of dry THF was added dropwise. The mixture was refluxed at 25°C for 24 h. After it was cooled to room temperature, the crude product solution was filtered and then concentrated by distillation under reduced pressure. Finally, the crude product was purified by hexane and put in a refrigerator overnight. We achieved a viscous, dark brown liquid by filtering the solution, and the yield was 72.33% (Scheme 1).

Synthesis of the AM/AA/AGE-TX-100 Copolymer

The copolymer was prepared by aqueous free-radical copolymerization. AM and AA were dissolved in deionized water in a 250-mL flask. Then, $NaHCO_3$ was used to control the pH value of the reaction solution between 6 and 8. After the mixture solution was stirred for 15 min, AGE-TX-100 was added to the reaction flask. The flask was purged with N_2 for 0.5 h. The reactant solution was then heated to the reaction temperature in a tempering kettle under a nitrogen atmosphere. An $(NH_4)_2S_2O_8$–$NaHSO_3$ initiator solution was added to the solution, and the polymerization proceeded for 24 h. The polymer was purified by precipitation with ethanol and dried in a vacuum oven at 40°C for 48 h (Scheme 2).

Measurement of the Intrinsic Viscosity

The intrinsic viscosity of the copolymer was measured with an Ubbelohde capillary viscometer at 30°C. The AM/AA/AGE-TX-100 copolymer was dissolved in distilled water, allowed to stand

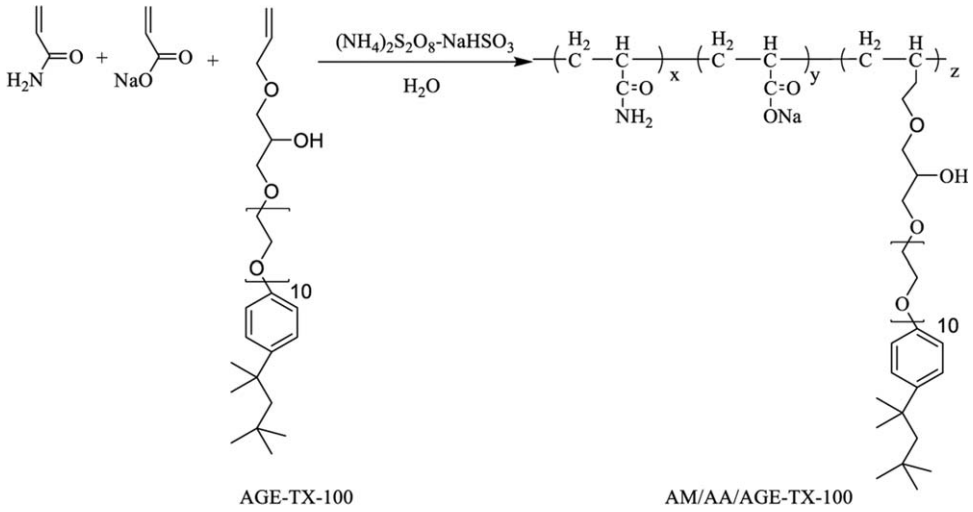

Scheme 2. Synthesis route for the AM/AA/AGE-TX-100 copolymer.

for 24 h, and then filtered to get rid of the insoluble material before testing. The copolymer solution was diluted by an NaCl solution to meet the required concentration, and the final concentration of NaCl in the copolymer solution was 1 mol/L. The concentrations of the copolymer solutions were changed from 1000 to 250 mg/L. The time it took for the liquid to pass through two calibrated marks was measured to describe the linear correlation between the relative viscosity (η_r) and the concentration.

η_r and the specific viscosity (η_{sp}) were determined as follows:

$$\eta_r = \frac{t}{t_0} = \eta_{sp} + 1$$

where t represents the flowing time of the copolymer solution and t_0 represents the flowing time of the 1 mol/L NaCl solution.

The intrinsic viscosity ($[\eta]$) was determined as follows:

$$[\eta] = \frac{H}{c}$$

where H represents the average of the y axis intercepts of the two corresponding regression lines and c is the concentration of the polymer solution (g/mL)

Fourier Transform Infrared Measurement

Fourier transform infrared spectra were recorded on a WQF-520 (PerkinElmer, Ltd., Beaconsfield Bucks, England) with samples as KBr disks. KBr pellets were prepared with the purified polymer powders.

^{1}H-NMR Measurement

^{1}H-NMR spectra were recorded at 400 MHz with an AM 400 spectrometer (Bruker, Switzerland) on samples to determine the structure of AGE-TX-100 and whether the AGE-TX-100 units were incorporated into the polymer molecules.

Solution Apparent Viscosity Measurement

Polymer solutions were prepared by the dissolution of the purified polymer in distilled water or aqueous salt solution. The apparent viscosities were measured by a Brookfield DVIII viscometer at the shear rate of 7.34 s^{-1}.

Rheological Measurement

The rheological properties of the polymer solution were measured by a Haake MARS III rotational rheometer. The correlation between the apparent viscosity and shear rate was achieved at 30°C via various shear rate from 0.01 to 1000 s^{-1}. The correlation between the apparent viscosity and temperature was obtained through changes in the temperature from 30 to 120°C under a constant shear rate (s^{-1}).

Environmental Scanning Electron Microscopy Measurement

The environmental scanning electron micrographs were made by a Quanta 450 environmental scanning electron microscope (FEI). All of the samples were dissolved in deionized water at the same concentration, and we put the samples at room temperature for 24 h before testing.

Emulsifying Abilities of the Surfmer and Polymer

The emulsifying ability of the copolymer was determined as follows. We prepared the polymer solutions by dissolving the nonionic surfmer AGE-TX-100, the cationic surfmer C_{16}DMAAC, the copolymer AM/AA/AGE-TX-100, the copolymer AM/AA/C_{16}DMAAC, HPAM, and the HPAM–surfactant system in deionized water to obtain the desired concentration of 2000 mg/L, whereas the blank sample was dissolved in the absence of polymer or surfmer. A 5-mL sample solution was stirred with an equal volumetric oil. After the solution was stirred for several minutes, the latex was charged into a 10-mL scale test tube, and we let it rest for a period of time (30 min for the surfmer test and 12 h for the polymer test). Then, the volume of the emulsion was recorded. All of the measurements were carried out at 25°C.

The emulsification activity was characterized by the emulsification index (EI), which was determined as the percentage height of the emulsified layer (in millimeters) divided by the total height of the liquid column (in millimeters) and was calculated as follows:

$$\mathrm{EI}(\%) = \frac{V_e}{V_t} \times 100\%$$

where V_e is the volume of the emulsion and V_t is the volume of the total solution.

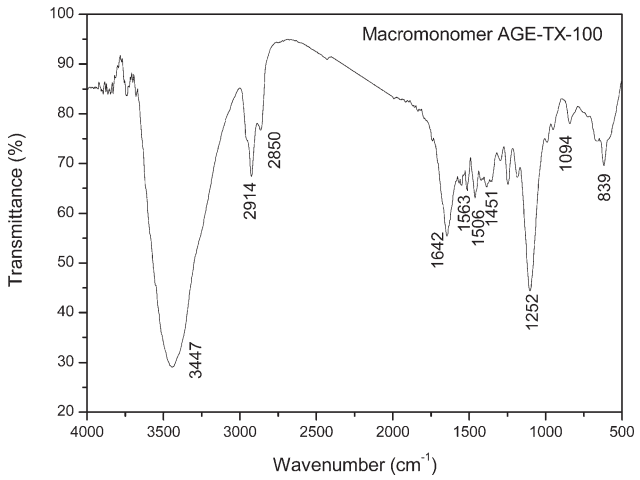

Figure 1. IR spectrum of the surfmer AGE-TX-100.

RESULTS AND DISCUSSION

Characterization of the Surfmer AGE-TX-100

Figure 1 shows the IR spectra of the surfmer AGE-TX-100. The absorptions at 3447, 2914, and 2850 cm^{-1} were due to the stretching vibrations of the —OH and —CH (—CH_2) groups. The peak at 1642 cm^{-1} was considered to be the —HC═CH_2 stretching vibrations. The absorption bands at 1563, 1506, 1451, and 839 cm^{-1} corresponded to the —HC═CH— stretching vibrations and bending vibrations in the aromatic ring. The peaks at 1252 and 1094 cm^{-1} indicated the presence of —HC═CH—O— and —C—O—C— groups.

The ^{1}H-NMR spectra of the surfmer AGE-TX-100 in $CDCl_3$ are shown in Figure 2: 0.71 (s, 9H, alkyl —CH_3), 1.33 (s, 6H, alkyl —CH_3), 1.69 (s, 2H, alkyl —CH_2), 1.84 (m, 2H, —CH_2O—), 3.60 (m, 40H, —CH_2CH_2O—, 2H, —CH_2O—, 1H, —CH—OH, 1H,—OH), 4.09 (t, 2H, —CH_2O—), 5.24 (m, 2H, C═CH_2), 5.87 (m, H, —CH═CH_2), 6.82 (d, 2H, —CH═CH— in the aromatic ring), and 7.25 (d, 2H, —CH═CH— in the aromatic ring).

These chemical shifts provided additional evidence to confirm the successful synthesis of the surfmer AGE-TX-100. The ^{1}H-NMR spectrum corresponded well with the IR spectrum.

Characterization of the AM/AA/AGE-TX-100 Copolymer

The IR spectra of the surfmer AGE-TX-100 [Figure 3(a)], AM [Figure 3(b)], and copolymer AM/AA/AGE-TX-100 [Figure 3(c)] are presented in Figure 3.

In Figure 3(c), the wide absorption at 3423 cm^{-1} was due to the —N—H and —O—H stretching vibrations. The peaks at 2923 and 2859 cm^{-1} were considered to be the stretching vibrations of the —CH_3 and —C—H (—CH_2—) groups. The peak at 1642 cm^{-1} was considered to be the —C═O stretching vibrations. The characteristic peak of the —CH_2CH_2O— group was

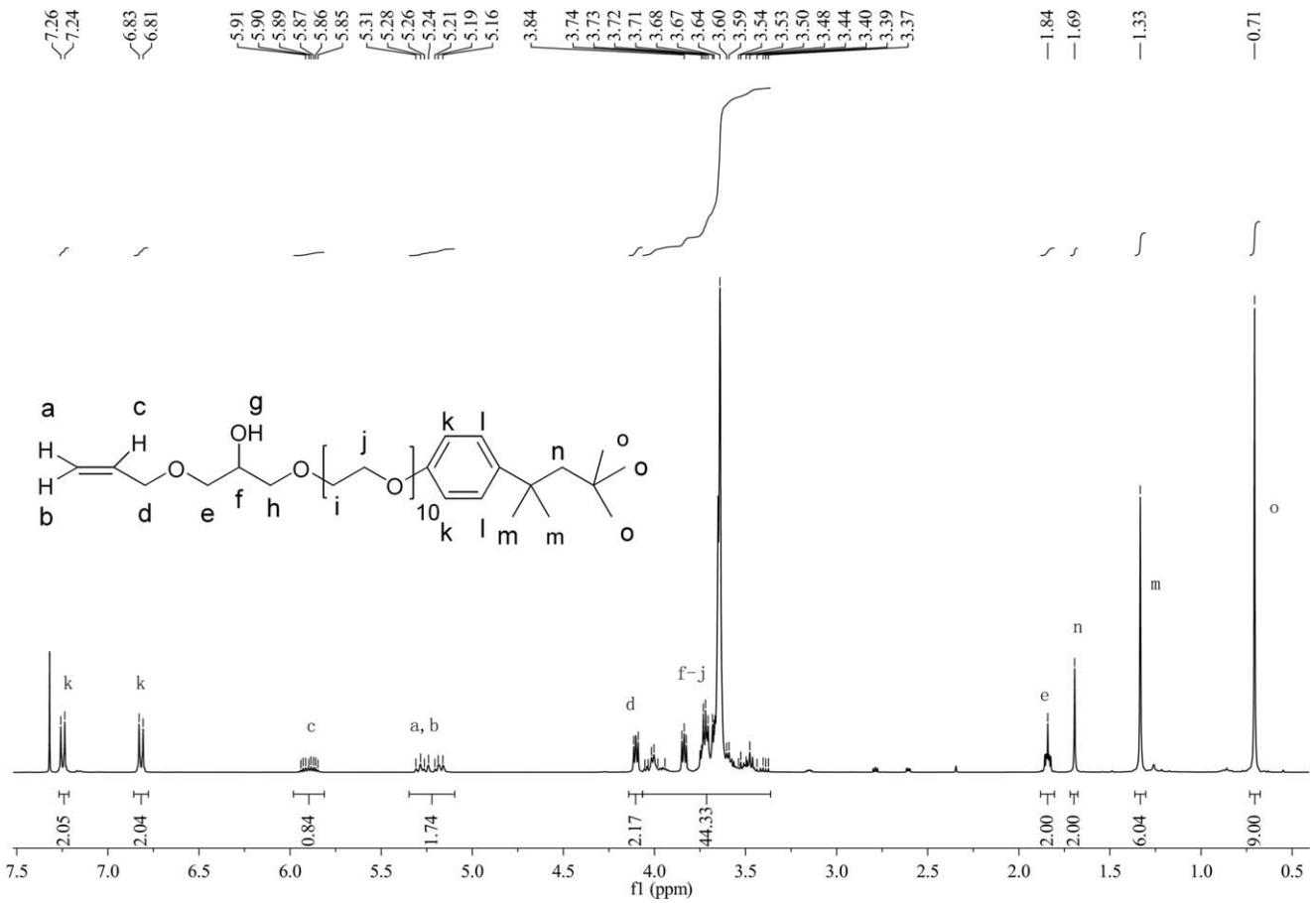

Figure 2. ^{1}H-NMR spectrum of the surfmer AGE-TX-100.

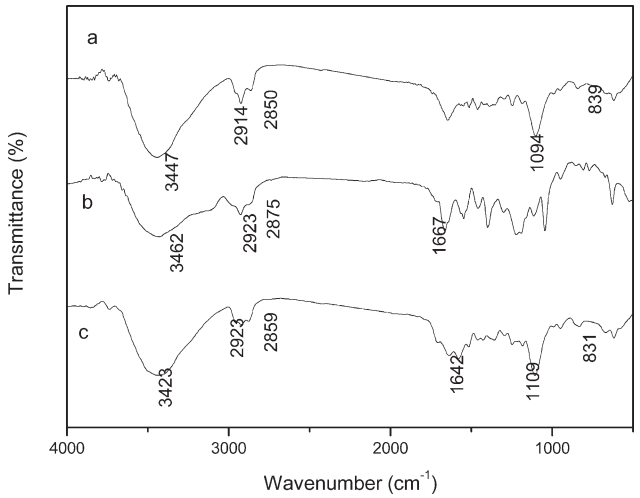

Figure 3. IR spectra of the (a) surfmer AGE-TX-100, (b) HPAM, and (c) AM/AA/AGE-TX-100 copolymer.

observed at 1109 cm^{-1}. The characteristic peak of the —HC═CH— bending vibration in the aromatic ring was evident at 831 cm^{-1}. These peaks mentioned previously for the copolymer AM/AA/AGE-TX-100 all corresponded well with the peaks of each monomer.

The ^{1}H-NMR spectra of the copolymer AM/AA/AGE-TX-100 is shown in Figure 4: 0.96–2.71 (the copolymer main chain and alkyl chain in TX-100), 3.41–4.29 (—CH_2CH_2O—, —CH_2O—, —CH—O—, —OH), 6.82 (—NH_2), and 7.63 (—CH═CH— in the aromatic ring).

The composition of the copolymer was analyzed further, and the degree of substitution for AGE-TX-100 groups in the copolymer AM/AA/AGE-TX-100 was determined according to the following equation:

$$\text{Hydrophobic group (mol\%)} = \frac{A_3}{A_1 + A_2 + A_3} \times 100\%$$

where A_1 is the integral area for the copolymer main chain and alkyl chain in TX-100; A_2 is the integral area for —CH_2CH_2O—, —CH_2O—, —CH—O—, and —OH; and A_3 is the integral area for —CH═CH— in the aromatic ring. The results are shown in Table I.

These chemical shifts provided additional evidence to confirm the successful copolymerization of AM, AA, and AGE-TX-100.

Optimization of the Reaction Conditions of the AM/AA/AGE-TX-100 Copolymer

As shown in Table II, the AM/AA/AGE-TX-100 ratios were investigated, and they are shown in entries 1–8. The results

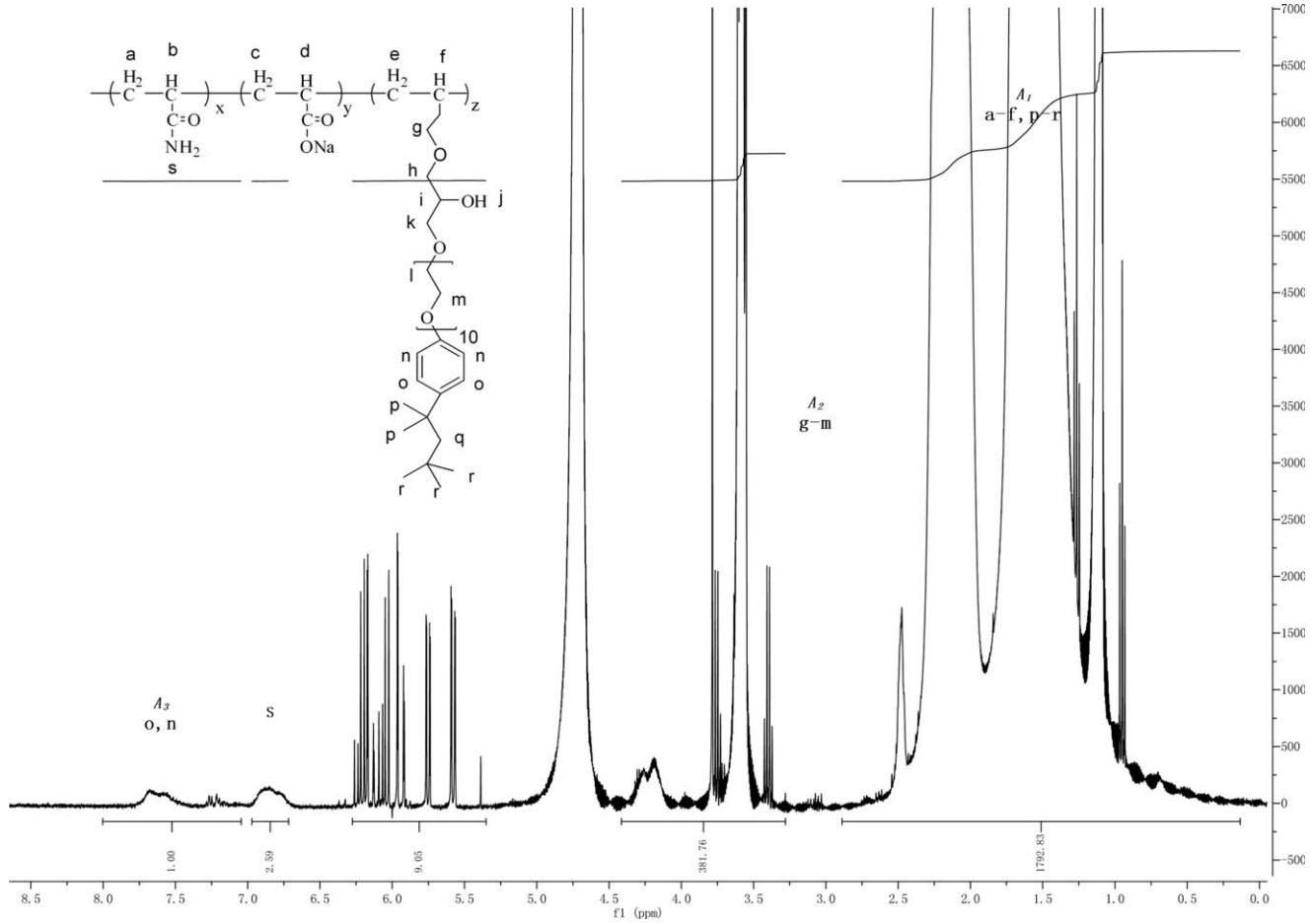

Figure 4. ^{1}H-NMR spectrum of the AM/AA/AGE-TX-100 copolymer.

Table I. Hydrophobic Degree of the AM/AA/AGE-TX-100 Copolymer

	Hydrophobic degree (mol %)		Hydrophobic degree (wt %)	
Copolymer	In the feed	In the copolymer	In the feed	In the copolymer
AM/AA/AGE-TX-100	0.056	0.050	0.06	0.053

indicate that the best AM/AA/AGE-TX-100 ratio was 7:3:0.06. After the ratio of AM/AA/AGE-TX-100 was optimized, the effect of the initiator was investigated. The data in entries 9–12 showed that the copolymer could achieve the best apparent viscosity (1667 mPa s) when the amount of initiator was 0.3 wt %. In addition, the reaction temperature and reaction time were both studied, as shown in entries 13–23. The results clearly show that the apparent viscosity of the copolymer solution reached 1645 mPa s when the reaction temperature was 45°C and the reaction time was 6 h. Compared with previous work,[44–46] experiments for selecting the emulsifiers and the optimization of the addition of emulsifiers did not need to be carried out, as AGE-TX-100, because of its amphiphilic structure, was not only a hydrophobic monomer but also a nonionic surfmer.

Intrinsic Viscosity of the AM/AA/AGE-TX-100 Copolymer

The flowing time was recorded with a stopwatch, and the test was repeated three times to get an average value. The flowing time of the 1 mol/L NaCl solution was 101.52 s, and the results of the copolymer are shown in Table III and Figure 5.

As shown in Figure 5, it was clear that the *y*-axis intercepts of the two corresponding regression lines were 0.84018 and 0.83388, and the average value of the *y*-axis intercepts was 0.83703. The intrinsic viscosity was calculated by the formulas, and it was 837 mL/g.

Effect of the Copolymer Concentration on the Apparent Viscosity

Figure 6 shows the influence of the polymer concentration on the apparent viscosity for the copolymer AM/AA/AGE-TX-100; copolymer AM/AA/C_{16}DMAAC, which contained a cationic surfmer structure as hydrophobic groups; and HPAM in aqueous solution. HPAM was synthesized without the addition of the hydrophobic monomer AGE-TX-100 under the same

Table II. Reaction Conditions of the AM/AA/AGE-TX-100 Copolymer

	Reaction conditions				Apparent viscosity (mPa s)[c]
Entry	$M_1/M_2/M_3$[a]	Initiator (wt %)[b]	Temperature (°C)	Time (h)	
1	9:1:0.03	0.5	45	24	873.5
2	8:2:0.03	0.5	45	24	1025
3	7:3:0.03	0.5	45	24	1200
4	6:4:0.03	0.5	45	24	781.6
5	5:5:0.03	0.5	45	24	641.3
6	7:3:0.06	0.5	45	24	1367
7	7:3:0.09	0.5	45	24	867.1
8	7:3:0.12	0.5	45	24	731.1
9	7:3:0.06	0.4	45	24	1402
10	7:3:0.06	0.3	45	24	1667
11	7:3:0.06	0.2	45	24	1025
12	7:3:0.06	0.1	45	24	—
13	7:3:0.06	0.3	30	24	726.7
14	7:3:0.06	0.3	35	24	985.1
15	7:3:0.06	0.3	40	24	1428
16	7:3:0.06	0.3	50	24	1201
17	7:3:0.06	0.3	55	24	1007
18	7:3:0.06	0.3	45	20	1686
19	7:3:0.06	0.3	45	15	1671
20	7:3:0.06	0.3	45	12	1665
21	7:3:0.06	0.3	45	8	1691
22	7:3:0.06	0.3	45	6	1645
23	7:3:0.06	0.3	45	4	921

[a] M_1, M_2, and M_3 represent the AM, AA, and AGE-TX-100 feed weight compositions, respectively. The monomer concentration was 20 wt %.
[b] $(NH_4)_2S_2O_8$-$NaHSO_3$ feed weight percentage with respect to the total monomers.
[c] The copolymer concentration in deionized water was 5000 mg/L; the measured conditions were 30°C and 7.34 s^{-1}.

Table III. Results of the Intrinsic Viscosity Tests for the AM/AA/AGE-TX-100 Copolymer

Entry	c^r	c (mg/L)	t (s)	η^r	η^{sp}	η^{sp}/c^r	ln η^r/c^r
1	1	1000	207.17	2.0407	1.0407	1.0407	0.7133
2	2/3	667	167.99	1.6547	0.6547	0.9821	0.7554
3	1/2	500	148.84	1.4661	0.4661	0.9322	0.7652
4	1/3	333	132.64	1.3065	0.3065	0.9195	0.8021
5	1/4	250	123.94	1.2208	0.2208	0.8834	0.7982

c_r, relative concentration of the copolymer solution.

reaction conditions as those used for the copolymer AM/AA/AGE-TX-100. The copolymer AM/AA/C_{16}DMAAC was synthesized with the same addition of C_{16}DMAAC at the same reaction conditions.

As shown in Figure 6, we found that the apparent viscosities of the copolymers increased with increasing concentration of the copolymers. The solution viscosity of the copolymer AM/AA/C_{16}DMAAC was much higher than the viscosity of the HPAM solution, but it was less than the viscosity of the copolymer AM/AA/AGE-TX-100 solution. Compared with the HPAM and copolymer AM/AA/C_{16}DMAAC, the copolymer AM/AA/AGE-TX-100 achieved a higher apparent viscosity at the same concentration; this indicated that the copolymer AM/AA/AGE-TX-100 exhibited a typical hydrophobic associative behavior in the aqueous solution. This was due to the small amount of amphiphilic groups of AGE-TX-100 in the side of the copolymer AM/AA/AGE-TX-100 chain. The critical association concentration of the copolymer AM/AA/AGE-TX-100 was 1000 mg/L, above which the apparent viscosity sharply increased with increasing polymer concentration.

Effect of Salts on the Apparent Viscosity

The salt-tolerance tests were carried out to investigate the polyelectrolyte behaviors of the copolymer AM/AA/AGE-TX in aqueous solution, and the results are shown in Figures 7–9.

As shown in Figures 7–9, it was clear that the apparent viscosities of the copolymer AM/AA/AGE-TX and HPAM decreased with increasing concentration of inorganic salts. Also, the apparent viscosities changed slightly when the concentrations of salts were above certain concentrations. This reflected the reduction in the dimensions of the polymer coils, which was due to the screening effect of the cations. As the cation concentration increased with increasing inorganic salts, the intra-anionic electrostatic repulsion in the polymer chain was sharply reduced, and the polymer chain began to shrink. This led to a loss of the apparent viscosity in the aqueous solution. The apparent viscosity was slightly changed as the addition of salts was completed to make the polyelectrolyte chain become a nonpolyelectrolyte chain. In addition, the salt-resisting tests showed that the viscosity of the polymer solution was sharply reduced with the addition of a low concentration of the multivalent ions Mg^{2+}

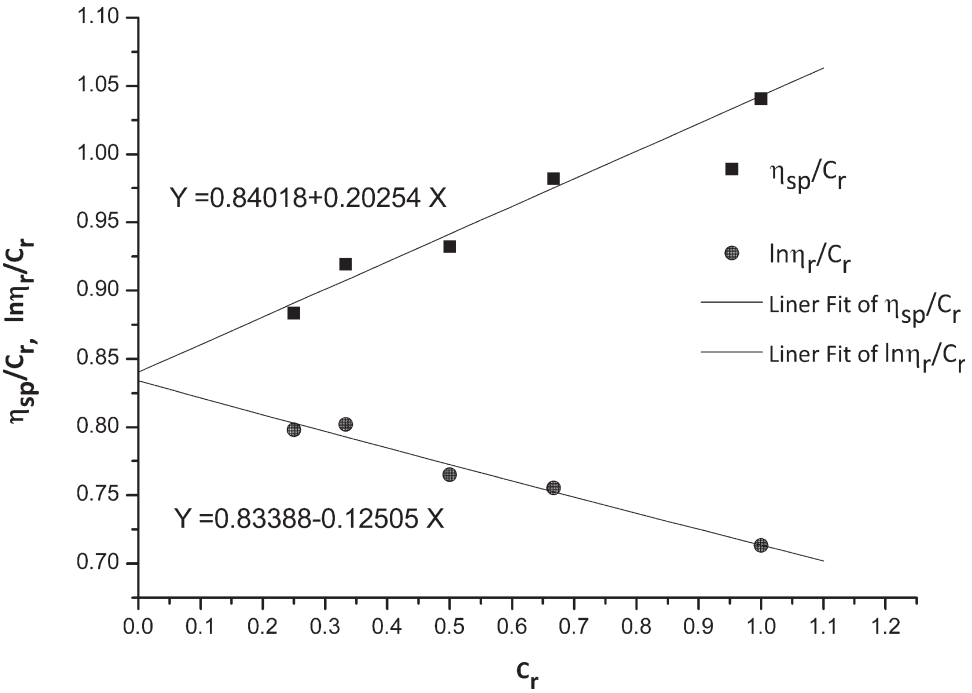

Figure 5. Liner correlation between η_r and c_r.

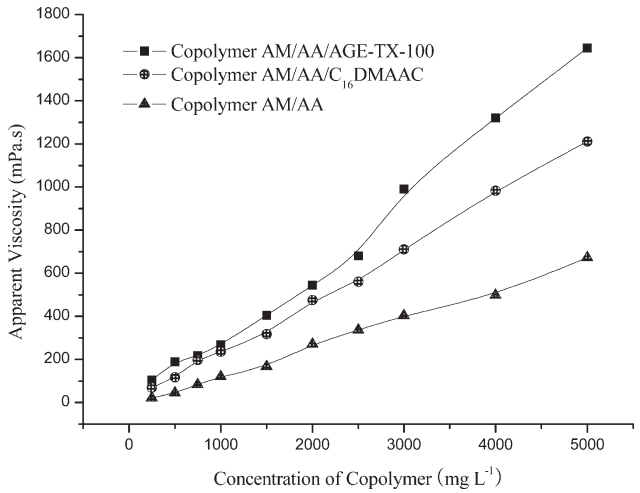

Figure 6. Effect of the copolymer concentration on the apparent viscosity at 25°C.

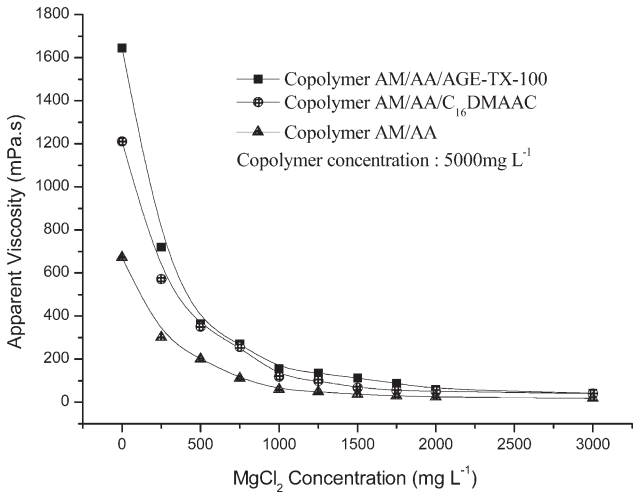

Figure 8. Effect of the $MgCl_2$ concentration on the apparent viscosity of the copolymer solution at 25°C.

and Ca^{2+}. This indicated that the multivalent ions Mg^{2+} and Ca^{2+} reduced the viscosity of the polymer solution more strongly than the univalent ion Na^{+}. This was due to the fact that the multivalent ions had stronger ionic strengths than the univalent ion, and they shielded the electrostatic charges on the polymer chains more effectively than the univalent ions, and this caused the reduction in the dimensions of the polymer chains.

Compared with the HPAM and copolymer AM/AA/C_{16}DMAAC, the copolymer AM/AA/AGE-TX-100 showed good salt tolerance and achieved a higher apparent viscosity at the same concentration of salts. The apparent viscosity reached 123.6 mPa s when the concentration of NaCl was 10,000 mg/L. The correlation of $MgCl_2$ and $CaCl_2$ had a similar tendency, and the apparent viscosities were 155.5 and 134.7 mPa s, respectively, when the concentration of salt was 1000 mg/L. This phenomenon might have been due to the small addition of the macromonomer AGE-TX-100 during the synthesis; it was introduced into the polymer chain, and this might have led to the intermolecular association of the copolymer in the salt solution. The molecular weight of the copolymer might also have made a big contribution to the viscosity. However, it was difficult to determine which, between the two factors, had a bigger influence on the viscosity of the copolymer because the molecular weight of the copolymer could not be determined by gel permeation chromatography nor by intrinsic viscosity. In addition, the copolymer AM/AA/C_{16}DMAAC also achieved a much higher viscosity than HPAM in the saltwater. However, the solution viscosity of the copolymer AM/AA/C_{16}DMAAC was less than that of the copolymer AM/AA/AGE-TX-100.

Effect of the Shear Rates on the Apparent Viscosity

The relationship between the shear rate and the apparent viscosity of the copolymer AM/AA/AGE-TX-100 was investigated through changes in the shear rate from 0.01 to 1000 s^{-1} at 30°C. The results are shown in Figure 10.

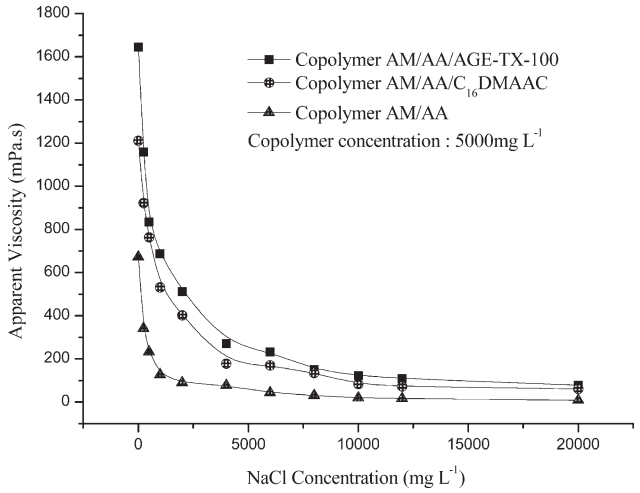

Figure 7. Effect of the NaCl concentration on the apparent viscosity of the copolymer solution at 25°C.

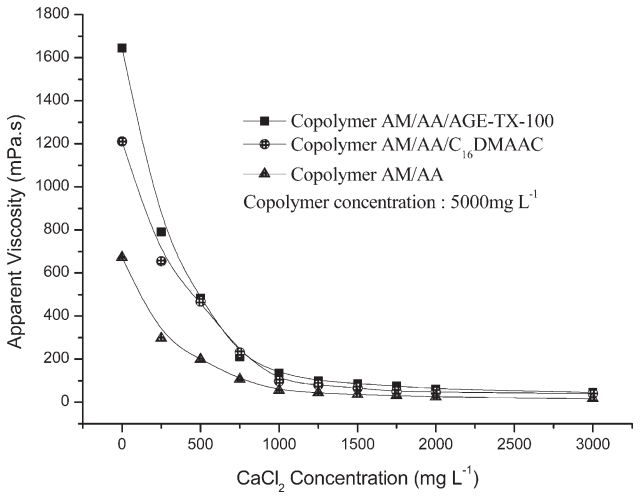

Figure 9. Effect of the $CaCl_2$ concentration on the apparent viscosity of the copolymer solution at 25°C.

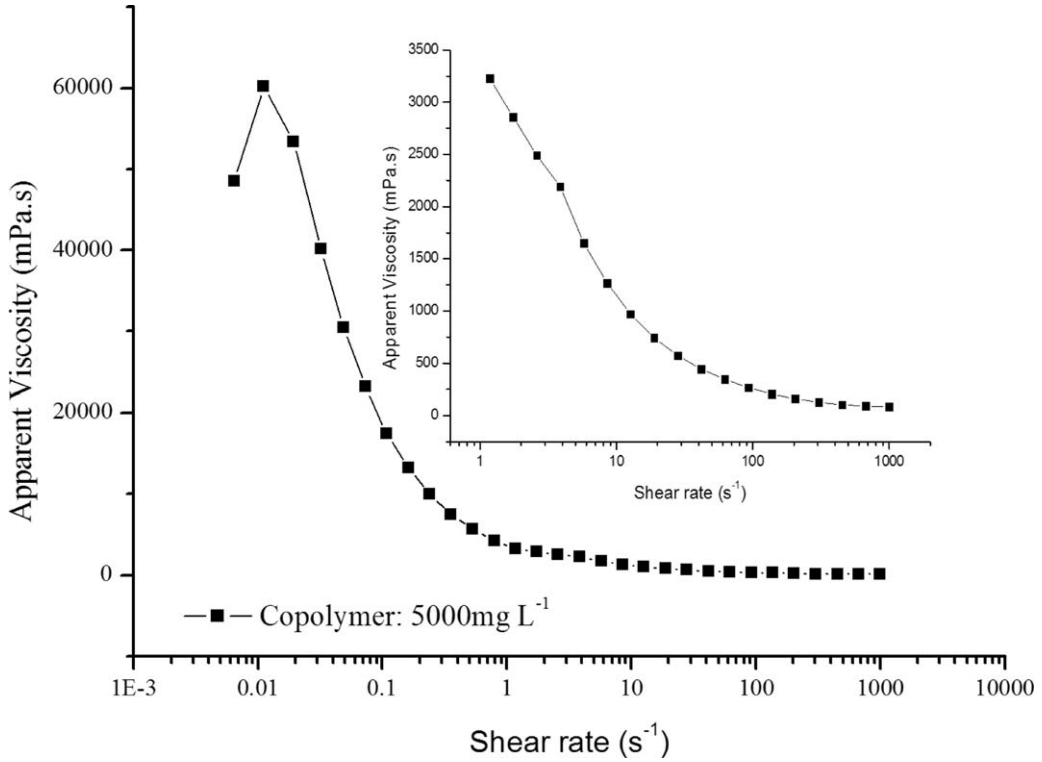

Figure 10. Effect of the shear rate on the viscosity of the copolymer solution.

As shown in Figure 10, it was clear that the apparent viscosity of the copolymer solution dramatically decreased from 60,136 to 265.52 mPa s with the increase in the shear rate from 0.01 to 92.35 s^{-1}. Then, with the continuing increase in the shear rate to 1000 s^{-1}, the apparent viscosity of the copolymer solution did not change obviously. The apparent viscosity of the copolymer solution remained at 206.29 mPa s at 137.39 s^{-1}. When the shear rate reached 1000 s^{-1}, the apparent viscosity of the copolymer solution was 88.87 mPa s. The results indicate that the copolymer AM/AA/AGE-TX-100 solution showed shear-thinning behavior and had a good shear resistance. In addition, this suggested that the molecules of the copolymer AM/AA/AGE-TX-100 associated in the aqueous solution to form a three-dimensional network that could build up a high viscosity at a low shear rate. As the shear rate increased, the motion diminished the entanglement of the copolymer molecules at a high shear rate, and this resulted in the breakage of the network structure and the reduction of the apparent viscosity. As the entanglement rate of the copolymer molecules was equal to the separation rate of the network structure, the apparent viscosity of the solution showed little change with increasing shear rate.

Effect of the Temperature on the Apparent Viscosity

The relationship between the temperature and the apparent viscosity of the copolymer AM/AA/AGE-TX-100 was investigated through changes in the temperature from 30 to 125°C at 170 s^{-1}. The results are shown in Figure 11.

Figure 11 shows that the apparent viscosity of the copolymer solution gradually decreased with increasing temperature, and there was no drastic reduction in the viscosity in the curve. The apparent viscosity was 100.02 mPa s at 100°C. When the temperature was continually increased to 125°C, the apparent viscosity was reduced to 47 mPa s. Then, when the temperature was kept at 125°C for 30 min, the apparent viscosity showed no obvious change. These results indicate that the temperature played a major role in controlling the viscosity of the copolymer solution and that the copolymer AM/AA/AGE-TX-100 had excellent shear stability at high temperatures. This could be explained by the motion of the polymer molecules. The rate of the polymer molecule motion increased with increasing temperature. The motion helped to build up a high viscosity by accelerating the association of the polymer molecules at low temperatures. On the contrary, the motion diminished the association of polymer molecules at high temperatures, and this

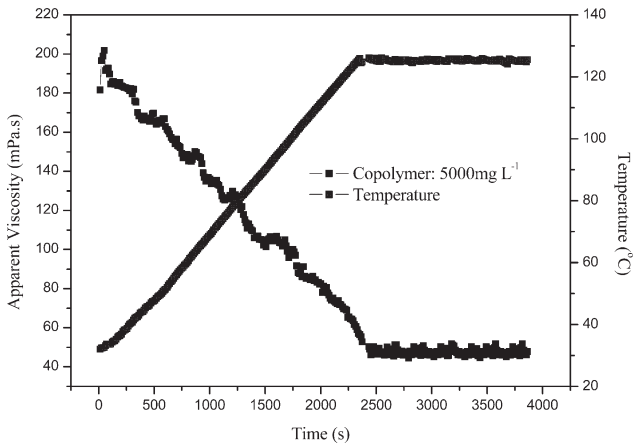

Figure 11. Effect of the temperature on the viscosity of the copolymer solution.

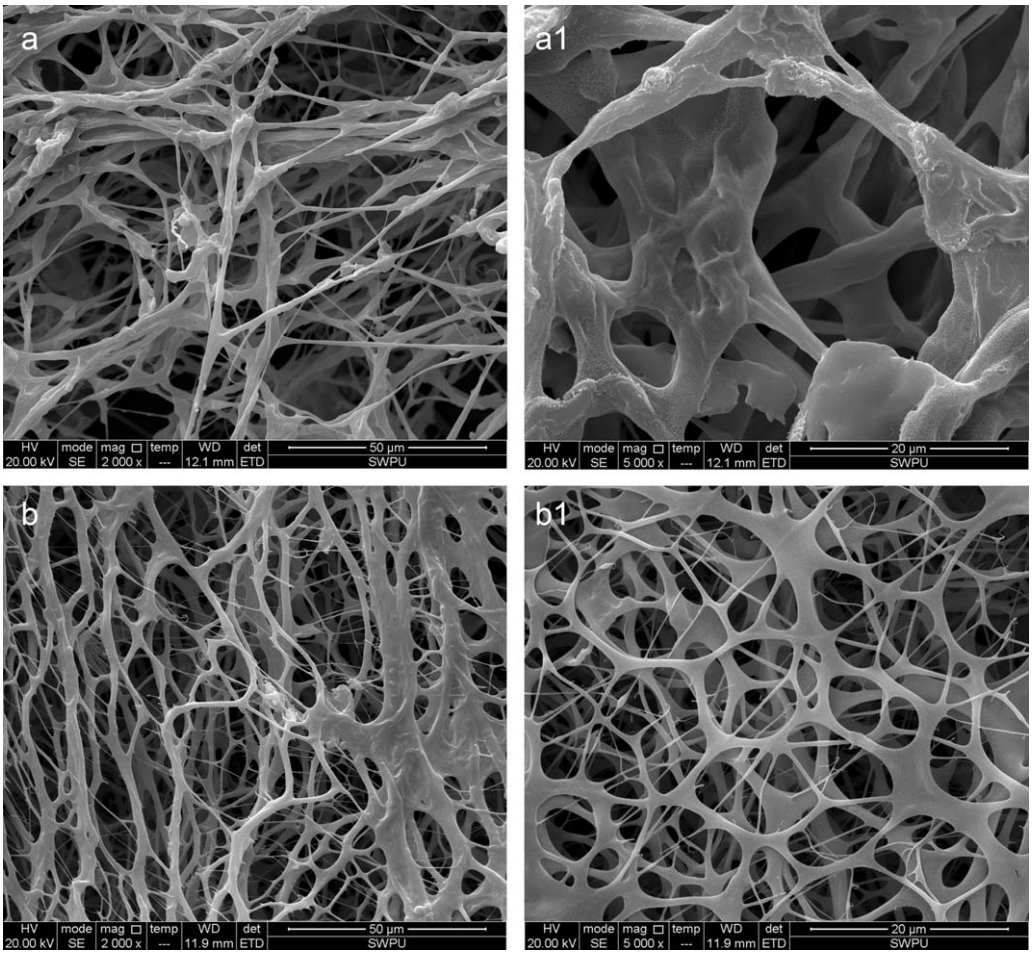

Figure 12. Environmental scanning electron micrographs of the (a) HPAM and (b) AM/AA/AGE-TX-100 copolymer.

resulted in breakage of the network structure and a reduction in the apparent viscosity. As the entanglement rate of the copolymer molecules surpassed the separation rate of the network structure, the apparent viscosity of the solution was decreased with increasing temperature.

Environmental Scanning Electron Micrographs of the Copolymers

The environmental scanning electron micrographs of the HPAM and copolymer AM/AA/AGE-TX-100 are shown in Figure 12. As shown in Figure 12(a), the microstructure of HPAM exhibited large open micropores or remained in a dispersed state. However, compared with the microstructure of HPAM, it was clear that the microstructure of the copolymer AM/AA/AGE-TX-100 was stronger and tighter, as shown in Figure 11(b). These pictures provide additional evidence for the intramolecular or intermolecular association of the copolymer AM/AA/AGE-TX-100 in aqueous solution, which was due to the small addition of amphiphilic groups of AGE-TX-100 to the side of the copolymer chains.

Analysis of the Emulsifying Abilities of the Surfmer and Polymer

In recent years, many laboratory tests and oil-field applications have confirmed that polymer flooding systems can increase oil recovery more notably than HPAM flooding systems because the former can emulsify crude oil during the EOR processes.[14,61,62] To better understand the solution properties of the surfmer AGE-TX-100 and copolymer AM/AA/AGE-TX-100 and explore their potential applications, emulsifying tests were carried out, and the results are shown in Figures 13 and 14 and Tables IV and V.

Figure 13 and Table IV show the experimental results of the surfmers for solubilizing and emulsifying petrol in aqueous solutions. The oil phase and water phase were separated completely in the case of the blank mixtures (without any surfmers), as shown in Figure 13(1). The results in Figure 13 show that both the cationic C_{16}DMAAC surfmer and nonionic surfmer AGE-TX-100 had good abilities for emulsifying petrol. However, compared with the cationic surfmer C_{16}DMAAC, the nonionic surfmer AGE-TX-100 showed better emulsification, and its EIs were 82% after 30 min and 60% after 12 h.

Figure 14 and Table V show the experimental results of solubilization and the emulsifying oil phase (petrol or crude oil) in aqueous solutions. The oil phase and water phase were separated completely in the case of the blank mixtures (without any polymers), as shown in Figure 14(a-1,b-1), whereas the oil/

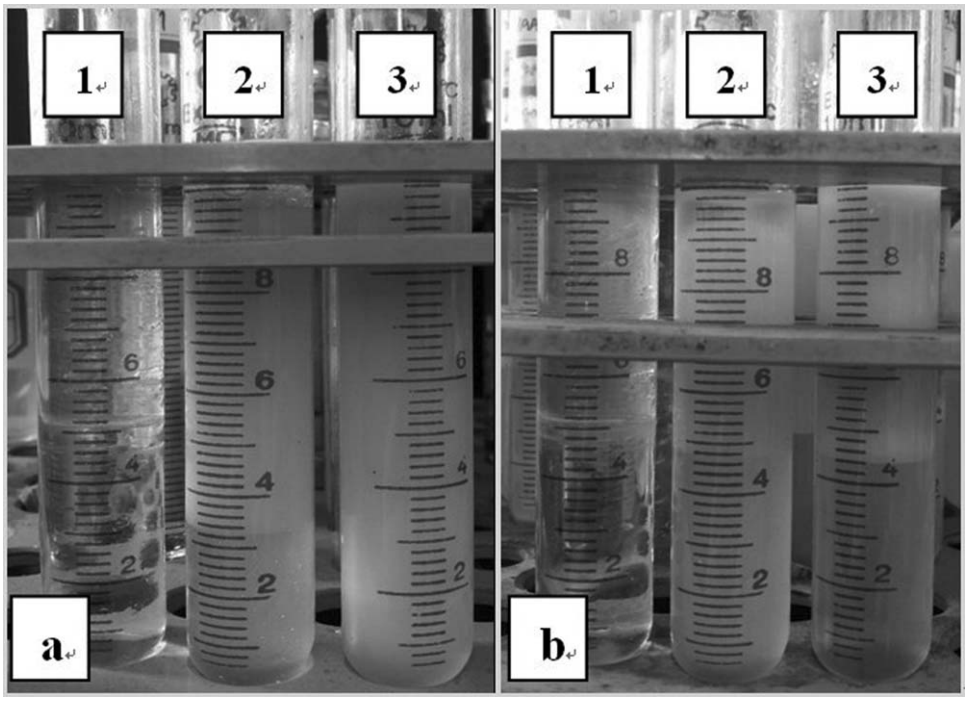

Figure 13. Photographs of surfmers for emulsifying petrol in water (a) after 30 min and (b) after 12 h: (1) blank sample, (2) 2000 mg/L C_{16}DMAAC, and (3) 2000 mg/L AGE-TX-100.

water interface became blurred [Figure 14(a-2,b-2)] for HPAM; this indicated the weak ability of HPAM to emulsify petrol and crude oil. As for the copolymer AM/AA/AGE-TX-100, the phase volume emulsified was larger than that in the HPAM system or the sodium dodecyl benzene sulfonate (HPAM-SDBS) system, and its EIs were 80% in the petrol sample and 64% in the crude oil sample. These observations suggest that the copolymer AM/AA/AGE-TX-100 had a good ability for emulsifying oil; this may result in a higher oil recovery than that in the HPAM system or the HPAM–SDBS system during the EOR processes. In addition, the solution of the copolymer AM/AA/C_{16}DMAAC also had the ability to emulsify petrol or crude oil like the copolymer AM/AA/AGE-TX-100. However, compared with the copolymer AM/AA/AGE-TX-100, the emulsion volume of the copolymer AM/AA/C_{16}DMAAC was smaller than that of the copolymer AM/AA/AGE-TX-100, and its EIs were 62% in the petrol sample and 60% in the crude oil sample after 12 h. This was probably due to the amphiphilic moieties of AGE-TX-100. Because the nonionic surfmer AGE-TX-100, with its TX-100 molecular structure (an excellent nonionic surfactant), had a better emulsifying ability than the cationic surfmer C_{16}DMAAC, it was introduced into the structure of the copolymer AM/AA/AGE-TX-100 as the side chain of the copolymer, and the copolymer AM/AA/AGETX- 100 displays the performance of polymeric surfactant in aqueous solution and could probably solubilize and emulsify organic components or mixtures.

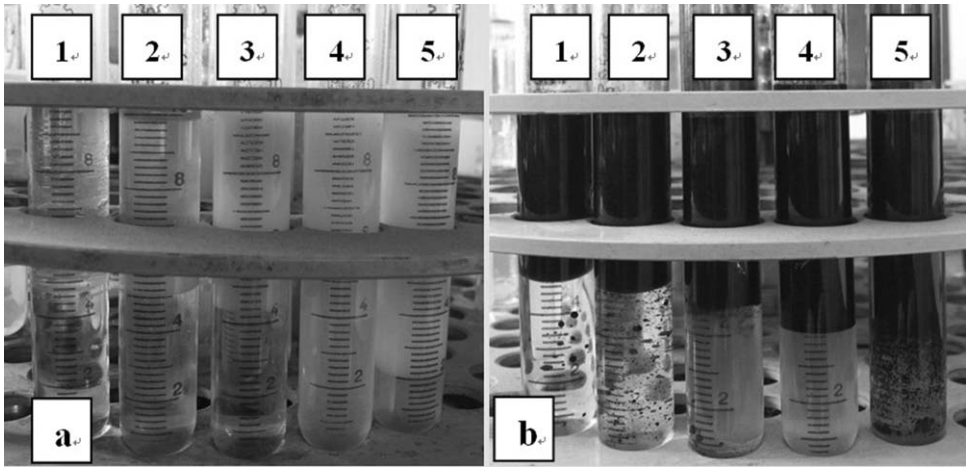

Figure 14. Photographs of polymers for emulsifying (a) petrol and (b) crude oil in water after 12 h: (1) blank sample, (2) 2000 mg/L HPAM, (3) 2000 mg/L HPAM and 2000 mg/L SDBS, (4) 2000 mg/L AM/AA/C_{16}DMAAC copolymer, and (5) 2000 mg/L AM/AA/AGE-TX-100 copolymer.

Table IV. Emulsification Activity Test of the Surfmers in a Stationary Emulsion

	EI after 30 min (%)			EI after 12 h (%)	
	Blank	C_{16}DMAAC	AGE-TX-100	C_{16}DMAAC	AGE-TX-100
Petrol	0	68	82	38	56

Table V. Emulsification Activity Test of Polymers in a Stationary Emulsion

	EI after 12 h (%)				
	Blank	HPAM	HPAM–SDBS	AM/AA/C_{16}DMAAC	AM/AA/AGE-TX-100
Petrol	0	27	56	62	80
Crude oil	0	27	54	60	64

Compared with the nonionic surfmer AGE-TX-100, the copolymer AM/AA/AGE-TX-100 sharply enhanced its emulsion stability. This may have been due to the viscosity of the copolymer solution because the emulsion viscosity improved the emulsion stability. However, compared with the cationic surfmer C_{16}DMAAC, the copolymer AM/AA/C_{16}DMAAC also improved its emulsion stability, but its EI after 12 h was less than that of the copolymer AM/AA/AGE-TX-100. This may have been due to the poor emulsion stability of the cationic surfmer C_{16}DMAAC. The results of the polymer emulsification test showed a good correlation with the previous results of the surfmer emulsification test

CONCLUSIONS

A novel surfmer, AGE-TX-100, was synthesized by the epoxide ring-opening reaction of allyl glycidyl ether and TX-100. Then, a novel copolymer, AM/AA/AGE-TX-100, was synthesized with AM, AA, and AGE-TX-100 in aqueous solution through free-radical random polymerization. The structures of the novel surfmer and copolymer were characterized by IR and ^{1}H-NMR. Compared with HPAM, the copolymer AM/AA/AGE-TX-100 showed good salt tolerance and achieved a higher apparent viscosity at the same concentration of salt. The apparent viscosity reached 123.6 mPa s when the concentration of NaCl was 10,000 mg/L. This might have been due to the small addition of AGE-TX-100 in the side of the polymer chain and the molecular weight of the copolymer. However, it is difficult to determine which made a bigger contribution to the viscosity of the copolymer between the two factors because the molecular weight of the copolymer could not be determined by gel permeation chromatography nor by intrinsic viscosity measurement. $MgCl_2$ and $CaCl_2$ had a similar tendencies, and their apparent viscosities were 155.5 and 134.7 mPa s, respectively, when the concentration of salt was 1000 mg/L. The rheological results show that the copolymer had a good thermal stability at high temperatures and a good shear resistance under high shear rates. The apparent viscosity of the copolymer solution was 100.02 mPa s at 100°C and was preserved at 88.87 mPa s when the shear rate was 1000 s^{-1}. The environmental scanning electron micrographs indicated that the copolymer formed a tighter three-dimensional network structure than HPAM in aqueous solution. In addition, the nonionic surfmer showed better emulsification than the cationic surfmer C_{16}DMAAC, and the copolymer had a good ability to emulsify organic components, which may increase oil recovery more than the HPAM flooding system or the HPAM–SDBS system during the EOR processes. More related research on the relationship between the viscosity, molecular weight, and macromolecular structure of the copolymer in the oilfield application of the copolymer AM/AA/AGE-TX-100 will be done in our future work.

ACKNOWLEDGMENTS

This work was financially supported by the Major National Science and Technology Program (contract grant number 2011ZX05024004). The authors thank the State Key Laboratory of Oil and Gas Reservoir Geology and Exploitation and the Engineering Research Center of Oilfield Chemistry (Ministry of Education Key Laboratory) for their support of these experiments.

REFERENCES

1. Thomas, S. Oil Gas Sci. *Technol. Rev. D* **2008**, *63*, 9.
2. Lake, L. W. *Oil Gas J.* **1990**, *88*, 62.
3. Donaldson, E. C.; Chilingar, G. V.; Yen, T. F. Enhanced Oil Recovery: Fundamentals and Analysis; Elsevier: Amsterdam, **1985**.
4. Taber, J. *J. Pure Appl. Chem.* **1980**, *52*, 1323.
5. Dandekar, A. Y. Petroleum Reservoir Rock and Fluid Properties; CRC/Taylor & Francis: Boca Raton, FL, **2006**.
6. Morrow, N. R. *J. Pet. Technol.* **1990**, *42*, 1476.
7. Ehrlich, R.; Wygal, R. *J. SPE J.* **1977**, *17*, 263.
8. .Energy Information Administration. U.S. Crude Oil, Natural Gas, and Natural Gas Liquids Reserves, 2002 Annual Report; Office of Oil and Gas, U.S. Department of Energy: Washington, DC, 2003.
9. Marilyn, R.; Bell, L. *Oil Gas J.* **2009**, *107*, 24.
10. Sheng, J. Modern Chemical Enhanced Oil Recovery: Theory and Practice; Gulf Professional: Amsterdam, **2011**.
11. Islam, M. R. *Energy Sources* **1999**, *21*, 97.

12. Lake, L. W. Enhanced Oil Recovery; Prentice Hall: Englewood Cliffs, NJ, **1989**.
13. Green, D. W.; Willhite, G. P. Enhanced Oil Recovery; SPE Textbook Series 1; Society of Petroleum Engineers: Richardson, TX, **1998**.
14. Sabhapondit, A.; Borthakur, A.; Haque, I. *Energy Fuels* **2003**, *17*, 683.
15. Wang, D.; Dong, H.; Lv, C.; Fu, X.; Nie, J. *SPE Reservoir Eval. Eng.* **2009**, *12*, 470.
16. Zhou, W.; Zhang, J.; Han, M.; Xiang, W.; Feng, G.; Jiang, W. Proceedings of International Petroleum Technology Conference (IPTC-11635); Dubai, U.A.E., 2007, p 1449.
17. Thomas, S.; Ali, S. M. F. *J. Can. Pet. Technol.* **1992**, *31*, 53.
18. Wang, H. Y.; Cao, X. L.; Zhang, J. C.; Zhang, A. M. *J. Pet. Sci. Eng.* **2009**, *65*, 45.
19. Shutang, G.; Qiang, G. SPE EOR Conference at Oil and Gas West Asia; Muscat, Oman, 2010; p 48.
20. Stoll, M.; Al-Shureqi, H.; Finol, J.; Al-Harthy, S. A.; Oyemade, S. N.; Kruijf, A. D.; Wunnik, J. N. M. V.; Arkesteijn, F.; Bouwmeester, R.; Faber, M. J. SPE EOR Conference at Oil and Gas West Asia, Muscat, Oman; SPE 129164; 2010; p 226.
21. Hernandez, C.; Chacon, L. J.; Anselmi, L.; Baldonedo, A.; Qi, J.; Dowling, P. C.; Pitts, M. *J. SPE Reservoir Eval. Eng.* **2003**, *6*, 147.
22. Manrique, E. J.; De Carvajal, G. G.; Anselmi, L.; Romero, C.; Chacon, L. J. *J. Pet. Technol.* **2001**, *53*, 51.
23. Manrique, E. J.; Thomas, C. P.; Ravikiran, R.; Kamouei, M. I.; Lantz, M.; Romero, J. L.; Alvarado, V. Presented at the SPE Improved Oil Recovery Symposium, Tulsa, OK, 2010; SPE 130113.
24. Bondor, P. L.; Hite, J. R.; Avasthi, S. M. Presented at the SPE Latin American and Caribbean Petroleum Engineering Conference, Rio de Janeiro, Brazil, 2005; SPE 94637.
25. Levitt, D. B.; Pope, G. A. *SPE Improved Oil Recovery Symp.* **2008**, *113845*, 1.
26. Peng, S.; Wu, C. *Macromolecules* **1999**, *32*, 585.
27. Seright, R. S.; Seheult, M.; Talashek, T. *SPE Reservoir Eval. Eng.* **2009**, *12*, 783.
28. Morgan, S. E.; McCormick, C. L. *Prog. Polym. Sci.* **1990**, *15*, 103.
29. Martin, F. D.; Hatch, M. J.; Shepitka, J. S.; Ward, J. S. *SPE Annu. Tech. Conf.* **1983**, *11786*, 1.
30. Pham, Q. T.; Russel, W. B.; Thibeaut, J. C.; Lau, W. *Macromolecules* **1999**, *32*, 5139.
31. McCormick, C. L.; Nonaka, T.; Johnson, C. B. *Polymer* **1988**, *29*, 731.
32. Hill, A.; Candau, F.; Selb, J. *Macromolecules* **1993**, *26*, 4521.
33. Jiménez-Regalado, E.; Selb, J.; Candau, F. *Macromolecules* **2000**, *33*, 8720.
34. Pancharoen, M.; Thiele, M. R.; Kovscek, A. R. *SPE Improved Oil Recovery Symp.* **2010**, *129910*, 1.
35. Buchgraber, M.; Clemens, T.; Castanier, L. M.; Kovscek, A. R. *SPE Annu. Tech. Conf.* **2009**, *122400*, 1.
36. Taylor, K. C.; Nasr-El-Din, H. A. *J. Pet. Sci. Eng.* **1998**, *19*, 265.
37. Lewandowska, K. *J. Appl. Polym. Sci.* **2007**, *103*, 2235.
38. Hu, Y.; Wang, S. Q.; Jamieson, A. M. *Macromolecules* **1995**, *28*, 1847.
39. Bradna, P.; Quadrat, O.; Dupuis, D. *Colloid Polym. Sci.* **1995**, *273*, 421.
40. Zhou, W.; Zhang, J.; Feng, G. Presented at the SPE Asia Pacific Oil and Gas Conference and Exhibition, Perth, Australia, 2008; SPE 115240.
41. Seright, R. S.; Seheult, M.; Talashek, T. *SPE Reservoir Eval. Eng.* **2009**, *12*, 783.
42. Feng, Y.; Billon, L.; Grassl, B.; Bastiat, G.; Borisov, O.; Francois, J. *Polymer* **2005**, *46*, 9283.
43. Guillaume, B.; Bruno, G.; Jeanne, F. *Polymer* **2005**, *289*, 359.
44. Wanli, K.; Yanfeng, J.; Bin, X. *Colloid Polym. Sci.* **2014**, *292*, 895.
45. Lanni, J.; Liangmin, Y.; Ru, L. *J. Appl. Polym. Sci.* **2013**, *130*, 1794.
46. Zhongbin, Y.; Mingming, F. *J. Appl. Polym. Sci.* **2013**, *130*, 2901.
47. Hill, A.; Candau, F.; Selb, J. *Macromolecules* **1993**, *26*, 4521.
48. Ye, L.; Luo, K.; Huang, R. *Eur. Polym.* **2002**, *36*, 1711.
49. Summers, M.; Eastoe, J.; Davis, S.; Du, Z. *Langmuir* **2001**, *17*, 5388.
50. Wu, H.; Kawaguchi, S.; Ito, K. *Colloid Polym. Sci.* **2004**, *282*, 1365.
51. Gao, B. J.; Guo, H. P.; Zhang, Y. *Macromolecules* **2008**, *41*, 2890.
52. Guyot, A. *Colloids Surf. A* **1999**, *153*, 11.
53. Huawei, W.; Seigou, K. *Colloid Polym. Sci.* **2004**, *282*, 13651.
54. Herold, M.; Brunner, H.; Tovar, G. E. M. *Macromol. Chem. Phys.* **2003**, *204*, 770.
55. Summers, M.; Eastoe, J. *Adv. Colloid Interface Sci.* **2003**, *100*, 137.
56. Hirai, T.; Watanable, T.; Komasawa, I. *J. Phys. Chem. B* **2000**, *104*, 8962.
57. Schoonbrood, H. A. S.; Unzue, M. J.; Asua, J. M. *Macromolecules* **1997**, *30*, 6024.
58. Stabler, K.; Selb, J.; Candau, F. *Mater. Sci. Eng. C* **1999**, *10*, 171.
59. Tuin, G.; Candau, F.; Zana, R. *Colloids Surf.* **1998**, *131*, 303.
60. Morimoto, H.; Hashidzume, A.; Morishima, Y. *Polymer* **2003**, *44*, 943.
61. Sun, J. L.; Sun, L. X.; Liu, W. D.; Liu, X. G.; Li, X.; Shen, Q. A. *Colloids Surf. A* **2008**, *315*, 38.
62. Samanta, A.; Ojha, K.; Mandal, A. *Energy Fuels* **2011**, *25*, 1642.